Rivas, E.; Barbero, E. (2016). Stiffness control in adaptive thin-walled laminate composite beams. *Composites Part A: Applied Science and Manufacturing*, v. 80, pp. 118-126.
https://doi.org/10.1016/j.compositesa.2015.10.016

Stiffness control in adaptive thin-walled laminate composite beams

E. Rivas, E. Barbero *

Department of Continuum Mechanics and Structural Analysis, University Carlos III of Madrid, Avda. de la Universidad 30, 28911 Leganés, Madrid, Spain

A B S T R A C T

The aim of this paper is to verify the control of the stiffness that is feasible to achieve in a thin walled box beam made from a laminate by including an adaptive material with variable stiffness. In this work, a material having a strongly varying Young Modulus under minor temperature changes was included in the cross section. An analytical model was used to estimate the position of shear centre and the axial, bending, torsional, and shear stiffnesses of the cross section. Two cross sections were analysed, one with an adaptive wall and another with two adaptive walls. In both sections, the torsional stiffness could be strongly altered with minor temperature variations. In the section with one adaptive wall, the shear centre and thus the bending twist coupling was also strongly modified. A study was made of the influ ence on the control of stiffnesses exerted by the overall cross section thickness and the thickness of the adaptive walls.

Keywords:
A. Laminates
A. Smart materials
C. Analytical modelling
C. Laminate mechanics

1. Introduction

The interest in developing new smart structures capable to self adapting to external stimuli that modify their shape or change their mechanical properties has increased considerably in recent decades. In this context, understanding and controlling the response of structures to the changes occurring in their environ ment is key to improving their performances.

The configuration of the structures can be controlled using different technologies, such as conventional mechanisms or com pliant mechanisms [1,2]. In some cases, mounted or embedded sensors need to be incorporated into the structures to provide them the ability to detect changes and take corrective actions [3].

One possible alternative is to control the configuration of a structure using materials having shape memory. These materials are able to remember their original shape and size and can recover it after being deformed after the application of an external condition, such as a temperature change [2].

Another alternative is the use of piezoelectric actuators, gener ally for shape control and vibration control of structures [3 6]. When mechanical loads are applied on a piezoelectric material, an electric field or a voltage is generated which is used to active shape and vibration control. On the other hand, the reverse effect also occurs: when an electric field or a voltage is applied to the piezoelectric material, it undergoes changes in stress and strains.

To meet the requirements of structures, a control technique that allows for great adaptability of the structure and its stiffness is necessary [2,7]. A variable stiffness material is one with elastic properties that can be controlled over time by varying some exter nal stimulus. If the variable stiffness material is part of a structure, the variation in its properties leads to a change in the properties of the overall structure. Such materials can be activated thermally, electrically, magnetically or chemically. These materials have great potential for use in aerospace structures. For example, Raither et al. [8], highlight the potential of shape adaptable airfoils for the control of the aerodynamic loads on wings by continuous deforma tions. Also, Gandhi and Kang [9] have studied the variation in the flexural stiffness of a multi layered beam when varying the tem perature of the polymer layers that formed it by applying heat with ultra thin electric heating blankets.

In many structural applications, i.e. aircraft structures, where weight is an important variable, thin walled structures are used, such as box beams for their great stiffness (especially the tor sional stiffness). Typical examples are wing spars and helicopter blades.

Not enough information is available in the scientific literature concerning box beams with walls made of a laminate when one or more walls are made from a variable stiffness material. Especially scarce is the information on the influence of the thick ness of the walls on the control of the beam stiffness of laminate box beams.

Isotropic beams have been analysed elsewhere [10], where the authors study a beam made of aluminium with a variable stiffness

* Corresponding author. Tel.: +34 916249965; fax: +34 916249430.
E-mail address: ebarbero@ing.uc3m.es (E. Barbero).

web. In another work [11], the authors examine an airfoil section made of composite material where several interfaces with controllable shear stiffness (PVC) are placed and the concept is based in variable bending twist coupling.

Raither [12] analysed a shape adaptable airfoil made of com posite material following an adaptive twist concept. The variable stiffness control in this study is based on two different systems: temperature control and voltage regulated control. This research contains a comparison between the elastic behaviour of composite variable stiffness beams (with elastic couplings) and the one of isotropic cross sections.

Several theories have been developed to estimate the stiffnesses and movements of thin walled composite beams by analytical models. However, an exhaustive review of such models is beyond the scope of the present paper. Smith and Chopra [13] have devel oped an analytical beam formulation to predict the effective elastic stiffness of tailored composite box beams, being aware of the advantages of this section. Kim and Shin [14] derive the shear stiff ness of a thin walled composite beam in several open section pro files. Volovoi and Hodges [15] predict the torsional stiffness of beams with closed sections of both a single cell and multi cell pro file. Pluzsik and Kollár [16] present a theory that takes into account the transverse shear and the restrained warping when calculating the bending and torsional stiffnesses of the section. Massa and Bar bero [17] developed a theory for the study of thin walled beams made from laminates and the calculation of the stiffnesses of sec tions of any geometry.

In present work the model proposed by Massa and Barbero [17] was used because it allows a variable stiffness material to be easily incorporated into the calculation of the stiffnesses of the thin walled composite beam. This analytical model is applicable to sec tions of different geometries, both open and closed, and thus offers the possibility of analysing different sections with relatively few modifications in the calculation process.

A phenomenon that appears in composite beams is the bend ing twist coupling or extension twist coupling. These couplings are caused partly by the anisotropy of composite materials, depending for example on the fibre orientation or the stacking sequence. Sometimes the coupling is undesirable, but on the other hand, these couplings appear to have great potential for various applications, prompting interest in the study of such problems. For example, the twist angle plays an important role in aerospace applications because it directly influences the angle of attack in air craft wings and helicopter blades [18]. For this reason, knowledge and quantification of couplings is crucial because, if they can be controlled or caused to an appropriate extent, they can contribute to the structural response of the beam. Some authors have studied the coupling phenomenon; for example, Raither et al. [1] have investigated the concept of adaptive bending twist coupling stiff ness of laminated composite plates based on the variation of shear stress transfer at layer interfaces.

The aim of the present paper is to determine the stiffness control that is possible to achieve in a thin walled box beam made from laminates when, due to a temperature variation, one of the walls undergoes a change in its properties. The variation of such properties, in addition to varying the stiffnesses of the sec tion, also causes a displacement in the position of the shear centre of the cross section and therefore results in a bend twist coupling that also has been studied because of the importance mentioned above. The thickness of a thin walled section is a relevant parameter in calculating cross section stiffness. For this reason, the global stiffnesses variation of the section (axial, bending, torsional, and shear) has been analysed when the thickness of the entire section and the thickness of the wall made of adaptive material vary.

2. Problem description

Two cross sections were analysed: a box section with one adaptive wall, Fig. 1a, and a section with the same overall geome try but with two adaptive walls, Fig. 1b. The first cross section allows an analysis of the case in which torsional stiffness under goes large variations associated with the change in properties of the adaptive material (i.e. when the temperature increases, the section behaves almost like an open section). The second cross section has lower shear stiffness due to the position of the adaptive walls, and thus the influence of temperature in the shear stiffness is high. The two sections have no variable stiffness flanges, since in some applications (as in aircraft structures) the principal bending stiffnesses should be affected as little as possible [10].

Variations in the adaptive material properties induce changes in the position of shear centre of the cross section, so that when a vertical load is applied at the shear centre at one temperature, a torque appears when the temperature changes.

For this reason the position of shear centre was also analysed. The reference case study corresponds to a temperature of 20 °C, and variations of ±20 °C with respect to the reference temperature have been considered. Higher temperature variations are difficult to reach in real applications.

The time course of the cross section stiffnesses with the change in adaptive material properties was studied. The axial stiffness, bending stiffness with respect to the principal axes of section, shear stiffness, and torsional stiffness were analysed. Also the dis placement of the shear centre was examined.

The adaptive material used is the elastomer Soundcoat Dyad 609 with a variation of the elastic constants taken from the literature [1]. A glass fibre/LY556 epoxy laminate with a $[0/90]_{2S}$ stacking sequence was selected. The mechanical properties of this composite material were taken from the literature [20].

In the present study, since the range of temperature variation is narrow, the variation of the composite material properties with temperature was not considered.

3. Analytical model

For the calculation of the stiffnesses of the thin walled beam, the model proposed by Massa and Barbero [17] was used. Because this paper examines the influence of the presence of the adaptive material in the beam response, hygrothermal effects on the composite material are not considered in the model formulation.

Each flat wall of the thin walled composite beam, which was a laminated plate, was described by one segment. Each had its corre sponding associated stiffness matrices and constitutive equations. If these equations are inverted and the undeformability of the con tour assumption of the classical theory of thin walled beams is applied together with the assumption of no coupling between nor mal and shearing effects [17], a reduced expression results, leading to the reduced constitutive equations of each i th segment in terms of the segment stiffness:

$$\begin{Bmatrix} N_x \\ M_x \\ N_{xs} \\ M_{xs} \end{Bmatrix}^i = \begin{bmatrix} A_i & B_i & 0 & 0 \\ B_i & D_i & 0 & 0 \\ 0 & 0 & F_i & C_i \\ 0 & 0 & C_i & H_i \end{bmatrix} \begin{Bmatrix} \varepsilon_x \\ \kappa_x \\ \gamma_{xs} \\ \kappa_{xs} \end{Bmatrix}^i \tag{1}$$

where the s axis and x axis define the laminate plane and the superscript i refers to each of the four segments. A description of the model and the variables used can be found in Massa and Bar bero [17]. In Eq. (1), A_i is the axial stiffness per unit length of the segment (in N/m), B_i is the coupling between bending curvature and extensional force (in N), D_i is the bending stiffness of the

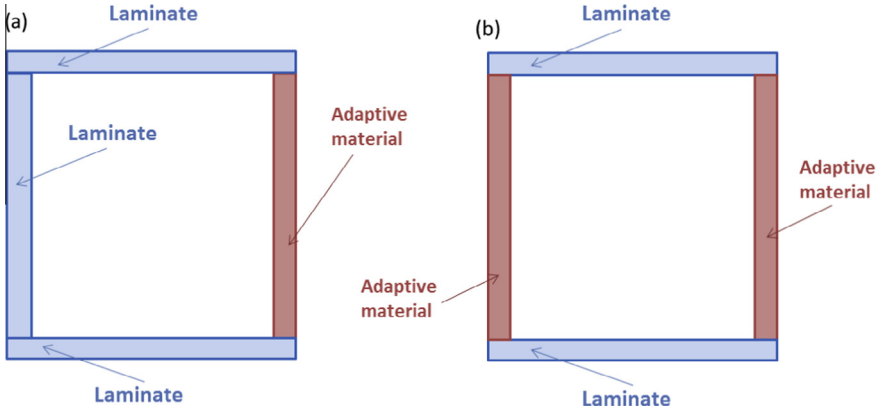

Fig. 1. Cross-sections used in the study. (a) One adaptive wall, (b) two adaptive walls. (For interpretation of the references to colour in this figure legend, the reader is referred to the web version of this article.)

segment under bending (in N m), F_i is the in plane shear stiffness under shear (in N/m), H_i is the twisting stiffness under twisting moment (in N m), and C_i is the coupling between the twisting curvature and the shear flow (in N). N_x, M_x, N_{xs}, and M_{xs} are the internal forces measured per unit length applied in each wall, while ε_x, K_x, γ_{xs}, and k_{xs} are the strains and curvatures of the laminate of each wall.

The global coordinate system used to define the stiffnesses is centred on the mechanical centre of gravity of the cross section and each laminate has a local coordinate system (s, r) where the s axis defines the width and the r axis defines the thickness of the laminate. The axial stiffness of the box section was determined by adding the contribution of all the segments, b_i being the i th segment length.

$$(\mathrm{EA}) \quad \sum_{i\ 1}^{n} A_i b_i \tag{2}$$

The bending stiffness is calculated with respect to the axes passing through the mechanical centre of gravity of the section. First, bending stiffnesses with respect to the principal axes of bending of each segment are calculated.

After this, a rotation is made in each segment in order to determine the bending stiffness with respect to a local coordinate system parallel to the global coordinate system of the section ($\mathrm{EI}^i_{y'}$ and $\mathrm{EI}^i_{z'}$). This angle is the one that each segment forms with respect to the global axes, 0° for the flanges and 90° for the webs in the case analysed.

Finally, with the use of parallel axis theorem and with the addi tion of the contribution of all the segments, the bending stiffness can be calculated with respect to the global axes of the section.

$$(\mathrm{EI}_{y_G}) \quad \sum_{i\ 1}^{n} \left[(\mathrm{EI}^i_{y'} + A_i b_i z_g^{i\,2} \right] \tag{3}$$

$$(\mathrm{EI}_{z_G}) \quad \sum_{i\ 1}^{n} \left[(\mathrm{EI}^i_{z'} + A_i b_i y_g^{i\,2} \right] \tag{4}$$

where z^i_g and y^i_g are the coordinates of the midpoint of each segment with respect to the global coordinate system centred in the mechanical centre of gravity (Y_G, Z_G).

The torsional stiffness is calculated by using the energy balance between the work done by an external torque and the strain energy due to shear. For the single cell closed section used in this study the torsional stiffness is:

$$(\mathrm{GJ}_R) \quad \frac{[2\Gamma_{s''}]^2}{\sum_{i\ 1}^{n} \frac{b_i}{F_i}} + \frac{3}{4}\left[4 \sum_{i\ 1}^{n} H_i b_i \right] \tag{5}$$

where $\Gamma_{s''}$ is the area enclosed by the midline of the contour of the section.

The shear stiffness can be determined by considering an infinitesimal element subjected to an arbitrary shear per unit length V_{ZG} and by using energy balance between the external work and the strain energy:

$$\mathrm{GA} \quad \frac{V_{ZG}^2}{\int_s \frac{q^2_{i(s)}}{F_i} ds} \tag{6}$$

where q_i (s) is the shear flow generated in the closed section due to the application of the load V_{ZG}. The integral of the denominator can be performed segment by segment for the study section.

For a calculation of the shear flow in each segment of the closed section, the shear flow must be calculated first as if the section were open at some point. This can be done by the expression in Eq. (7).

$$q_i\ (\mathrm{s}) \quad \frac{V_{ZG} \cdot \mathrm{EQ}_{YG}\ (\mathrm{s})}{\mathrm{EI}_{YG}} \tag{7}$$

where EQ_{YG} (s) is the mechanical static moment of the i th segment defined in [17,19].

It should be noted that the shear V_{ZG} appears as a constant in the calculation of shear flows (Eq. (7)). Therefore, in the calculation of shear stiffness (Eq. (6)), its contribution is cancelled because it appears in both the numerator and denominator. It is necessary to find a constant shear flow so that adding it to the shear flow of the open section results in the shear flow of the closed section. Such shear flow is calculated assuming that the load V_{ZG} is applied in the shear centre of the section and therefore the torsional rota tion is zero.

Once the shear flow in the real closed section is known, the position of the shear centre of the section can be determined by the equilibrium of moments about any point, under the assump tion that V_{ZG} is applied at the shear centre.

4. Model validation

No experimental results of adaptive composite beams were found in the scientific literature, and therefore the model accuracy was analysed with experimental movements of aluminium beams, as reported by Raither et al. [10]. These authors present experi mental data on cantilever beams with a box section, with three walls made of aluminium and the fourth (one of the webs) of a PMMA polymer. The geometry of the experimental beams used in the present study is shown in Fig. 2b. The experimental cross section cannot be reproduced precisely by the model, and thus a simplified cross section was considered (Fig. 2a).

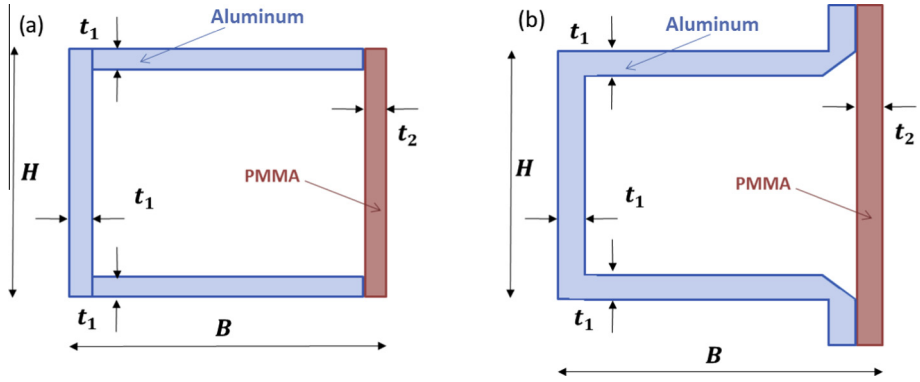

Fig. 2. Cross-section used in model validation. (a) Simplified geometry, (b) experimental geometry [9]. (For interpretation of the references to colour in this figure legend, the reader is referred to the web version of this article.)

The beam was subjected to two point load cases at the free end, 21.91 N (Load case A) and 33.95 N (Load case B). The load was applied at the geometric centre of the cross section, which is different from the shear centre, so that a bending twist coupling appears. Thus, in addition to the bending rotation and vertical displacement, a torsional rotation was measured.

The movements determined from the analytical model, i.e. the vertical displacement and bending rotation at the free end of the beam, were estimated using the classical equations of Strength of Materials for a cantilever beam subjected to a point load on the free end. For the estimation of the torsional rotation, a simplified formulation that does not consider warping was used. The vertical displacement and torsional rotation and the free end of the beam, and calculated by the analytical model were compared with those in Ref. [10] and are listed in Table 1.

The analytical model quite accurately predicted both move ments for the two load cases analysed. The observed differences may have arisen because the geometry of the experimental cross section is slightly different from the geometry used in the analytical model, Fig. 2.

Since no additional information was found in the scientific liter ature to validate the model experimentally, a numerical simulation was made to verify the results of the analytical model. The move ments at the end of a cantilever beam considering the section shown in Fig. 1a and the geometry data of Table 2 were estimated with both the numerical and analytical model. A load equal to 1 N was applied at the free end of the beam, and in the shear centre at 20 °C. A $[0/90]_{2S}$ glass fibre/LY556 epoxy laminate was analysed. The mechanical properties of this material are taken from Ref. [20].

Abaqus/Standard was used to model the beam using four node shell elements (S4R in Abaqus nomenclature). The clamped end of the beam was modelled by constraining all degrees of freedom of the corresponding nodes. The exact point where the load was applied (the shear centre at 20 °C) was located outside the section and defined as a reference point linked as a rigid body to the sec tion at the free end of the beam. The point load was applied at this point.

The movements of the free end of the beam were determined directly from the numerical analysis as the movements of the reference point. This is because the rigid body constraint allows restriction of the motion of the free end to the motion of the refer ence point. On the other hand, the analytical movements were esti mated using Strength of Materials equations.

Table 1
Results of the model validation: analytical and experimental [9].

		Load case A	Load case B
Vertical displacement	Analytical (mm)	1.018	1.578
	Experimental (mm)	1.123	1.782
	Differences (%)	9.79	11.50
Torsional rotation	Analytical (rad)	1.304	2.021
	Experimental (rad)	1.446	2.206
	Differences (%)	9.79	8.41

Table 2
Beam geometry for the model validations.

Validation	Parameters				
	H (mm)	B (mm)	t_1 (mm)	t_2 (mm)	L (mm)
Validation with experimental results from Raither et al. [9]	38	80	1	1	800
Validation with numerical simulation	50	30	3	3	1000

As reflected in Fig. 3, good agreement was found between the numerical and analytical results. Percentage changes between the two models relative to the vertical displacement are very small, 0.97% at 40 °C and 0.14% at 0 °C. The bending rotation estimation provided by the analytical model was virtually identical to the numerical one, the differences being less than 0.008% for the entire temperature range selected. Percentage changes between the results of the analytical model and the numerical model related to torsional rotation were 8.9% at 0 °C and 16.2% at 40 °C.

The differences in the torsional rotations at 40 °C were good, as can be seen in Fig. 3, but not as good as those for vertical displace ment and bending rotation, due to the simplicity of the model used to estimate the rotation. One reason for largest difference may be that the movements due to warping were not included in the ana lytical formulation. For this reason the model, in the actual formu lation, are only applicable to small temperature changes. However, even with small changes in temperatures, significant variation of rotation can be achieved (Fig. 3).

Since the differences were minor with both the experimental and numerical results, it can be stated that the analytical model accurately predicts the stiffnesses of the beam when the adaptive properties of the material changes.

5. Results

5.1. Control of movements by the adaptive material

The variation in the stiffnesses of section with temperature for the two sections studied was calculated (Fig. 1a and b), using the geometry shown in Table 2, second row. The thicknesses of the walls of both laminate and adaptive material were 3 mm. All global stiffnesses values were lower in the section with two adap tive walls than in the section with one adaptive wall, due to the

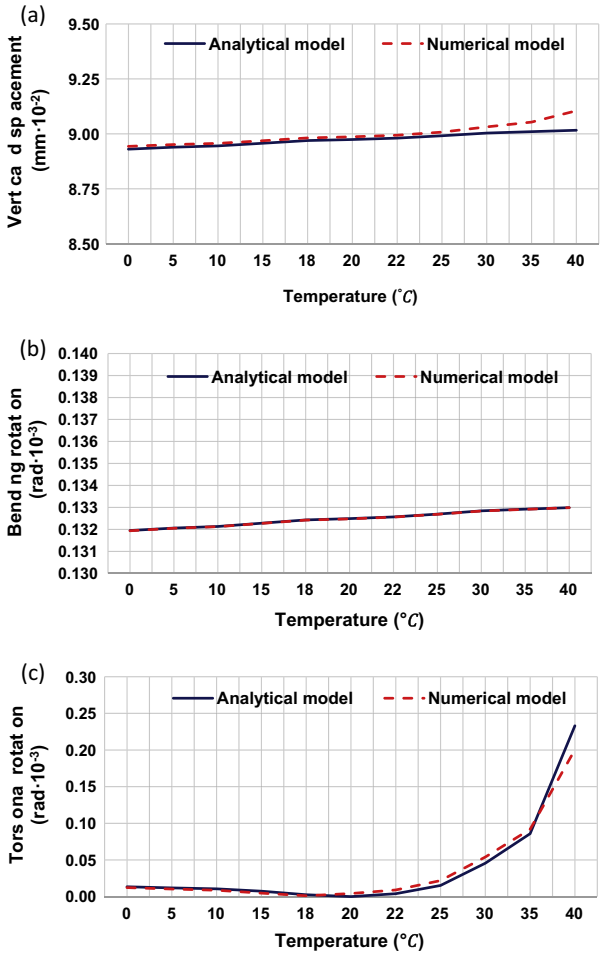

Fig. 3. Comparison between analytical and numerical simulations, (a) Vertical displacement, (b) Bending rotation, (c) Torsional rotation. (For interpretation of the references to colour in this figure legend, the reader is referred to the web version of this article.)

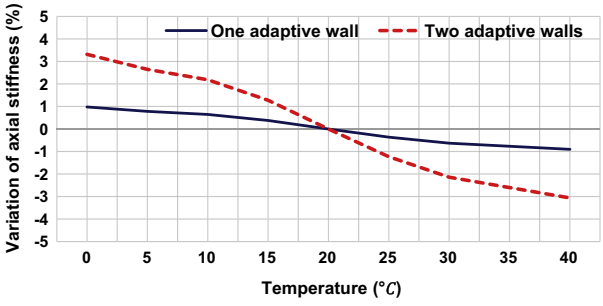

Fig. 4. Axial stiffness variation (%) with respect to the reference temperature for the two cross-section analyzed. (For interpretation of the references to colour in this figure legend, the reader is referred to the web version of this article.)

lower Young Modulus of the adaptive material than the composite material. For a comparison of the behaviour of both sections when temperature changed from 0 °C to 40 °C, the percentage variation of the section stiffness and the position of the shear centre with respect to the reference value at 20 °C were calculated (Figs. 4 8).

The influence of temperature was greater in the cross section with two adaptive walls than in the section with one adaptive wall in the axial, bending, and shear stiffnesses, Figs. 4, 5 and 7. This is because the section with two adaptive walls had a higher

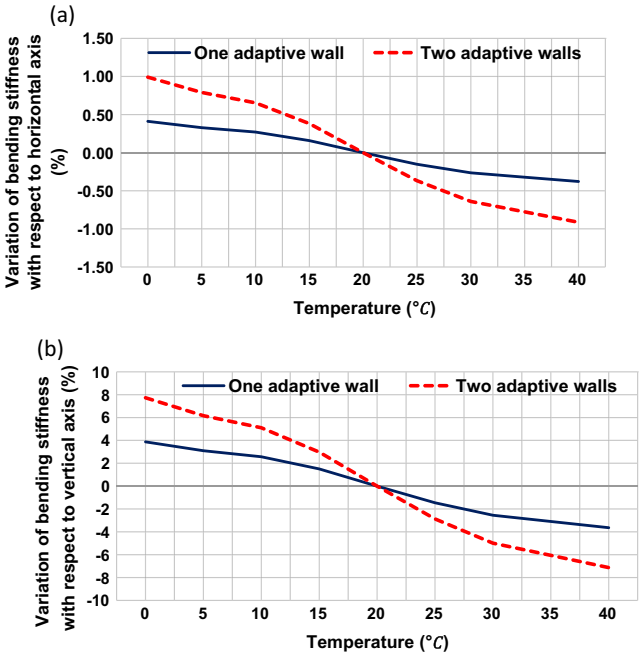

Fig. 5. Bending stiffness variation (%) with respect to the reference temperature for the two cross-sections analyzed. (a) With respect to horizontal axis, (b) With respect to vertical axis. (For interpretation of the references to colour in this figure legend, the reader is referred to the web version of this article.)

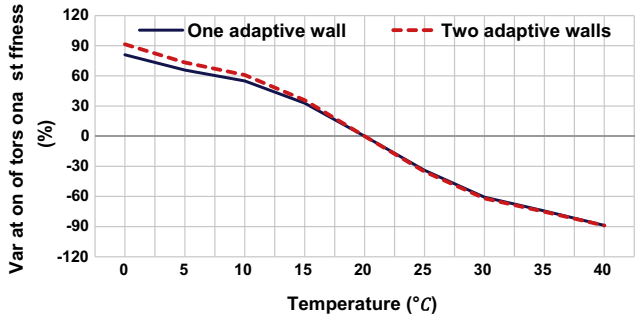

Fig. 6. Torsional stiffness variation (%) with respect to the reference temperature for the two cross-sections analyzed. (For interpretation of the references to colour in this figure legend, the reader is referred to the web version of this article.)

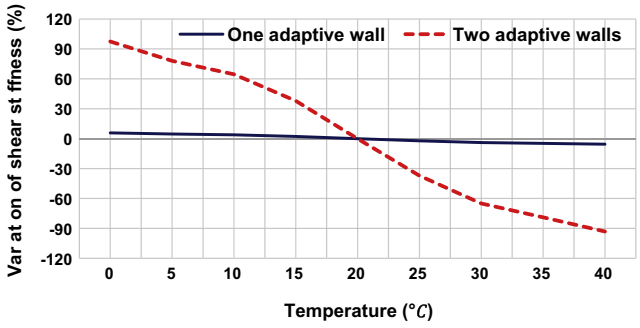

Fig. 7. Shear stiffness variation (%) with respect to the reference temperature for the two cross-sections analyzed. (For interpretation of the references to colour in this figure legend, the reader is referred to the web version of this article.)

proportion of adaptive material having properties (Young Modu lus) that varied heavily with temperature. This also happened in the section with one adaptive wall, but in this case the stiffness variation with the temperature was lower.

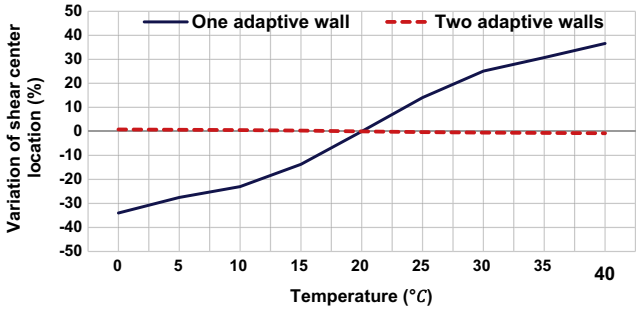

Fig. 8. Shear centre variation (%) with respect to the reference temperature for the two cross-sections analyzed. (For interpretation of the references to colour in this figure legend, the reader is referred to the web version of this article.)

The variation with temperature of axial stiffness and bending stiffness around the horizontal axis were small (Figs. 4 and 5a), and therefore it was not possible to control these types of stiffness by an adaptive material for the sections studied in this work. In the best case, a variation of the axial stiffness of about 3% for the section with two adaptive walls can be achieved and only a variation of less than 1% in the case of the section with one adaptive wall. The variation of the bending stiffness around the horizontal axis was less than 1% for the two sections in the temperature range selected.

Due to the location of the adaptive wall in both cross sections, the variation of the bending stiffness with respect to vertical axis was higher than the other bending stiffness (Fig. 5b). For the section with two adaptive walls the maximum variation was more than 7% at 40 °C, and therefore the control achieved by introducing the adaptive material in the section was greater for this type of stiffness.

By contrast, the torsional stiffness was strongly altered when the temperature was changed, varying from about 90% for a temperature variation of only 20 °C in both sections (Fig. 6). As a result, the torsional stiffness and therefore the torsional rotation could be controlled by the addition of an adaptive material to the cross section. The variation of the torsional stiffness according to temperature proved similar in both cross sections, unlike bending and axial stiffnesses, in which the variation significantly differed. This different behaviour was due to the formulation of the torsional stiffness compared to that of the axial and the bending stiffnesses. In the first case, the contribution to torsional stiffness of the stiffness of each segment (F_i) was in the denominator (Eq. (5)), the stiffness of each segment (A_i) appearing in the numerator in the calculation of bending stiffnesses of the cross section (Eqs. (3) and (4)).

In the cross section with two adaptive walls, the shear stiffness was significantly lower than in the section with one adaptive wall. At 20 °C the stiffness of the first one was 82.37 kN and 706.02 kN for the second one (the stiffnesses used in this work are defined per unit length). The low shear stiffness of the section with two adaptive walls made the contribution of shear force in the transversal displacement relevant. Also, the shear stiffness of this section was strongly altered by temperature. For both reasons, even though the bending stiffness was not significantly altered, it was possible to control the transverse displacement by means of the adaptive material. For example, for a cantilever beam subjected to a point load at the free end, the transversal displacement can be modified by around 138% with a variation of 20 °C.

The position of shear centre was modified to the case of the section with one adaptive wall up to 36% (Fig. 8). This allowed the bending twist coupling to be controlled by introducing an adaptive material. The shear centre in the cross section with two adaptive walls was not altered by the temperature due to the symmetry of this section.

5.2. Influence of thickness in the variation of stiffness

The influence that wall thickness exerts on the control of section stiffnesses was investigated when the properties of the adaptive material changed with temperature. Two studies were made: in the first one, the thicknesses of all walls of the section were changed uniformly, and in a second study, only the thickness of the adaptive wall was changed. The study section was formed by three walls of composite and one wall of adaptive material Fig. 1a.

5.2.1. Influence of the cross section thickness

Sections with four different wall thicknesses of 0.5, 1, 3, and 5 mm were studied. The other geometries of the section are those shown in Table 2, second row. The upper limit of the wall thickness was selected at 5 mm so that the section may be considered thin walled, and thereby ensure that the analytical model assumptions would be valid. The lower limit of the wall thickness was selected at 0.5 mm so that the variation studied was by one order of magnitude.

When the section was made thicker by between 0.5 and 5 mm, the stiffness value of the section increased 8 to 10 fold at the reference temperature. However, although the stiffness values changed significantly with changes in wall thickness of the section, the influence of such change on the stiffness control with temperature was not as important, Figs. 9 12. An increase in the thickness of the section slightly diminished the influence of temperature in the variation of all stiffnesses. This was because greater thickness of all section walls caused the walls made of composite material to become more rigid and therefore it became more difficult to determine the variation of the overall stiffness of the section with the adaptive material in the configuration analysed.

For instance, at a temperature of 40 °C, the shear stiffness of the section 0.5 mm thick was equal to 0.108 MN (stiffness per unit length), while the shear stiffness corresponding to the Section 5 mm thick was equal to 1.158 MN (Stiffness per unit length). For the first thickness, the variation with respect to the shear stiffness at the reference temperature was 5.8%, while this value slightly decreased to 5.33% at 5 mm thick (Fig. 12). This result was similar for the axial and torsional stiffnesses, (Figs. 9 and 11). In the case of the bending stiffness about the main axes, the influence of the wall thickness in controlling stiffness with temperature was reduced to a greater extent, approximately threefold.

A wall thickness increase of one order of magnitude between 0.5 mm and 5 mm raised the value of the axial stiffness per unit length of each segment (A_i) by one order of magnitude. However, the bending stiffness of each segment (D_i) was boosted by three

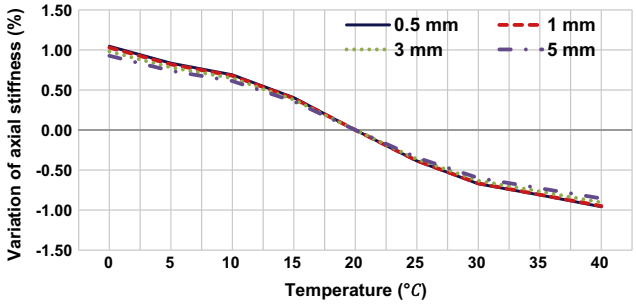

Fig. 9. Axial stiffness variation (%) with respect to the reference temperature for several cross-section thicknesses. (For interpretation of the references to colour in this figure legend, the reader is referred to the web version of this article.)

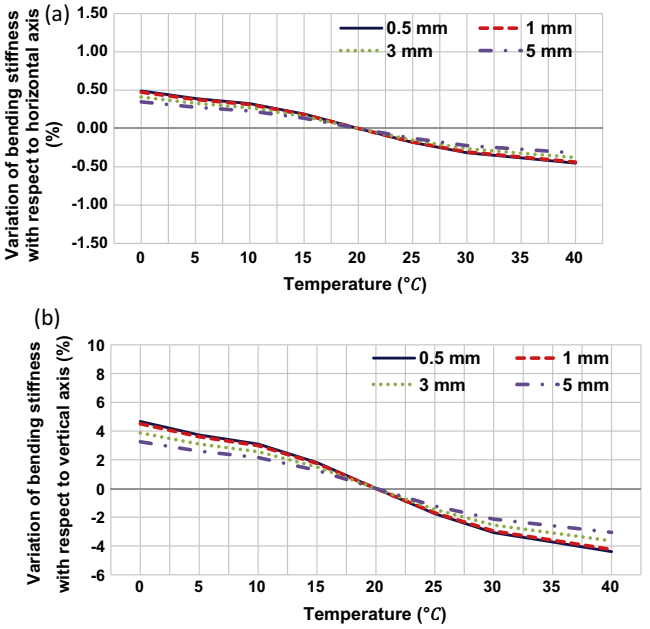

Fig. 10. Bending stiffness variation (%) with respect to the reference temperature for several cross-section thicknesses. (a) With respect to horizontal axis, (b) with respect to vertical axis. (For interpretation of the references to colour in this figure legend, the reader is referred to the web version of this article.)

orders of magnitude when the thickness was increased. The axial stiffness of the cross section was controlled exclusively by the A_i of each wall. On the other hand, for the section analysed, the bend ing stiffness of the cross section with respect to the horizontal axis was controlled by the D_i of the flanges and the A_i of the webs. Since the flanges were made of composite material, their properties could not be controlled with temperature. This made the ability to control EI_{y_G} of the cross section lower than the ability to control EA when the section thickness was increased. Similar reasoning explains the behaviour of EI_{z_G}.

The influence of section thickness in the position of the shear centre was not as significant as in the case of the stiffnesses. At 20 °C the shear centre of the section of 0.5 mm thickness was located outside the section, at a distance of 8.19 mm from the left web, while it was located at 6.34 mm in the case of 5 mm thick ness. In the numerator of the expression, for calculating the shear centre, relationships appeared between shear flows that increased by 7 to 8 fold when the thickness was increased, but also in the denominator appeared the bending stiffness that changed signifi cantly, too, as stated above. These effects were counteracted to some extent, which explains the weaker influence of the thickness in the shear centre position. The influence of the thickness in con trolling the shear centre position after temperature changes was negligible (Fig. 13). Thus, for the first thickness, a temperature increase of 20 °C shifted the position of the shear centre by 36.92% relative to the position at the reference temperature. This change was 36.32% for the thickness of 5 mm (Fig. 13). It was found that the change in the shear flows of the section with temperature was practically independent of the thickness of the section.

5.2.2. Influence of the thickness of the adaptive wall

The variations in the cross section stiffnesses and the shear centre position with the temperature were analysed, when the thickness of the wall of adaptive material changed. The thickness of the other walls were kept constant at 1 mm. Thicknesses of 1, 3, and 5 mm were studied, selecting the upper limit to ensure that the section could be considered thin walled.

The increase in thickness of the adaptive material of the wall slightly incremented the axial, bending, and shear stiffnesses of the cross section for temperatures below the reference tempera ture. Above the reference temperature the influence on these stiff nesses of the wall of adaptive material was negligible since the Young Modulus of adaptive material was very small. The control of axial, bending, and shear stiffnesses significantly increased by between 2.5 and 4 fold when thicknesses of the adaptive wall increased (Figs. 14, 15 and 17). This was because greater amounts of adaptive material in the section allowed greater control over these stiffnesses.

The thicker wall of adaptive material made it possible for a thickness of 5 mm to control the EI_{z_G} by up to 15% and the shear stiffness by 20%. Because both types of stiffnesses allow control of the movement of the beam, it is possible to exercise a non negligible control over the transverse displacement by means of the adaptive material for the study section with walls of this thickness.

The torsional stiffness took higher values when increasing the thickness of the wall of adaptive material. Thus, for the reference temperature, torsional stiffness increased from 37.13 N m^2 for a thickness of 1 mm in the wall made of adaptive material, to 120.18 N m^2 for a thickness of 5 mm. This is because when the stiffness of the wall made of adaptive material is very low, the sec tion behaves like an open section, and therefore has very low tor sional stiffness. With a thicker wall of adaptive material, torsional stiffness of the section augments because its behaviour is that of a closed section. The ability to control the torsional stiffness by means of the adaptive material was very high, reaching 90%. However, a thicker wall of adaptive material slightly diminished the ability to control this stiffness at temperatures below the refer ence temperature (Fig. 16). Moreover, at temperatures above the reference temperature, the stiffness of the adaptive material was

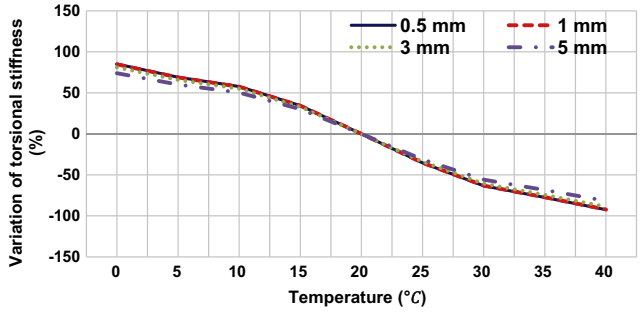

Fig. 11. Torsional stiffness variation (%) with respect to the reference temperature for several cross-section thicknesses. (For interpretation of the references to colour in this figure legend, the reader is referred to the web version of this article.)

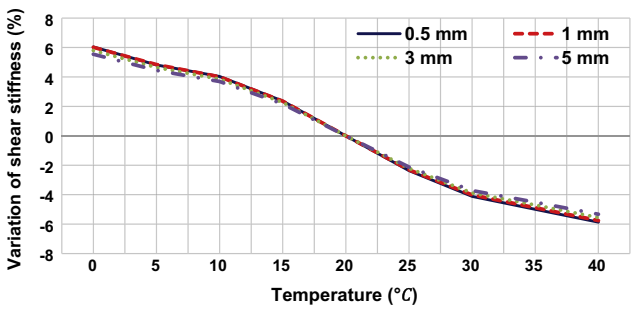

Fig. 12. Shear stiffness variation (%) with respect to the reference temperature for several cross-section thicknesses. (For interpretation of the references to colour in this figure legend, the reader is referred to the web version of this article.)

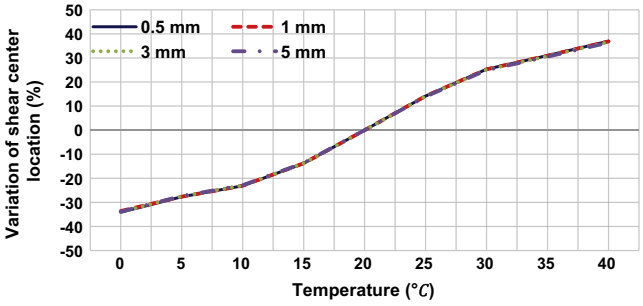

Fig. 13. Shear centre variation (%) with respect to the reference temperature for several cross-section thicknesses. (For interpretation of the references to colour in this figure legend, the reader is referred to the web version of this article.)

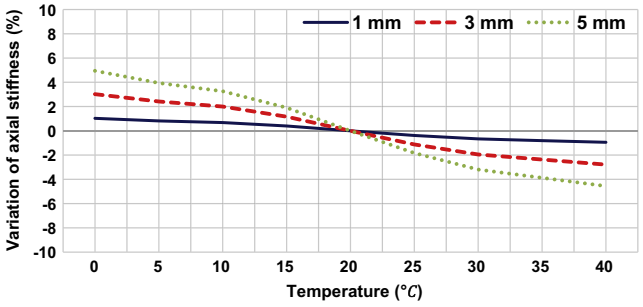

Fig. 14. Axial stiffness variation (%) with respect to the reference temperature for several thicknesses of the adaptive wall. (For interpretation of the references to colour in this figure legend, the reader is referred to the web version of this article.)

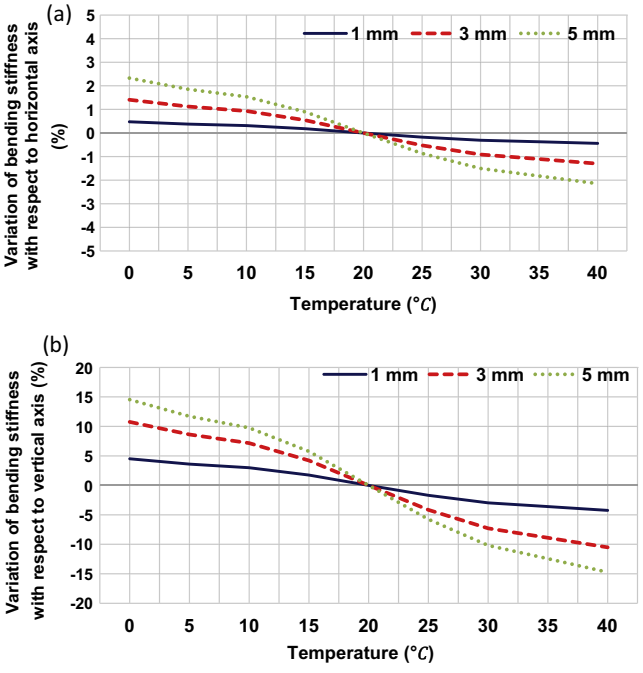

Fig. 15. Bending stiffness variation (%) with respect to the reference temperature for several thicknesses of the adaptive wall. (a) With respect to horizontal axis, (b) with respect to vertical axis. (For interpretation of the references to colour in this figure legend, the reader is referred to the web version of this article.)

so low that there was no influence of the thickness in the ability to control this stiffness.

The variation in the position of the shear centre was strongly influenced by the wall thickness of adaptive material. It went from

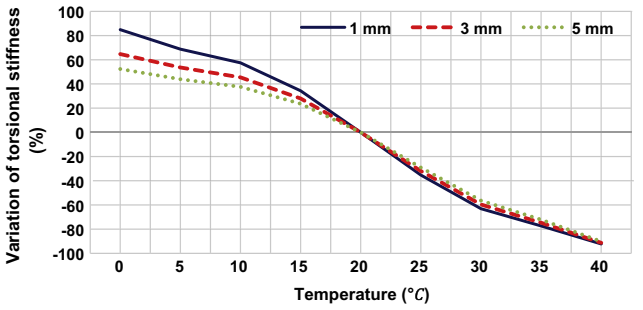

Fig. 16. Torsional stiffness variation (%) with respect to the reference temperature for several thicknesses of the adaptive wall. (For interpretation of the references to colour in this figure legend, the reader is referred to the web version of this article.)

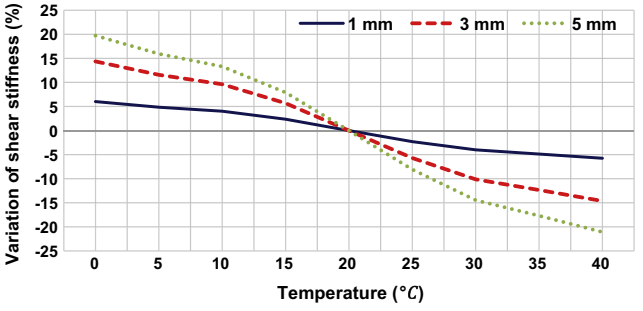

Fig. 17. Shear stiffness variation (%) with respect to the reference temperature for several thicknesses of the adaptive wall. (For interpretation of the references to colour in this figure legend, the reader is referred to the web version of this article.)

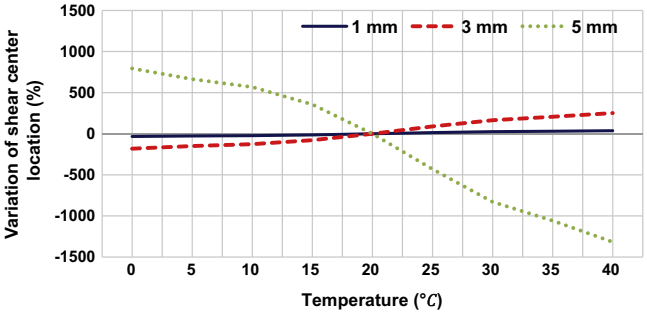

Fig. 18. Shear centre variation (%) with respect to the reference temperature for several thicknesses of the adaptive wall. (For interpretation of the references to colour in this figure legend, the reader is referred to the web version of this article.)

changing at about 37% for a thickness of 1 mm when the tempera ture is shifted, to changing by more than 1300% for a thickness of 5 mm (Fig. 18). In all the cases the location of the shear centre was measured from the left web of the cross section.

Therefore, the thickness of the wall made of adaptive material constitutes a key parameter for controlling the bending twist coupling in a thin walled composite beam.

6. Conclusions

By means of an analytical model, this paper analyses the effects of including an adaptive material with variable stiffness to control the stiffnesses, and thus the displacement and rotations, of a thin walled composite box beam. This model was validated by experi mental results and a numerical simulation. Two cross sections were studied, one with an adaptive wall and another with two adaptive walls.

The results for both sections analysed in this paper show that the control of torsional stiffness in a composite box section by including an adaptive material is very high. The stiffness control therefore allows control of the twists due to torsional moments. By contrast, the control that can be achieved on the axial and bend ing stiffnesses is limited. The differences in the behaviour of the torsional stiffness relative to the other ones are due to the different formulation of this stiffness.

All stiffnesses values of the section with two adaptive walls were lower than in the section with only one adaptive wall due to the low Young Modulus of the adaptive material. The ability to control the axial, bending, and torsional stiffnesses of the section with two adaptive walls was similar to that of the other section, but somewhat higher. However, in this section the shear stiffness was strongly altered. Due to the low shear stiffness of the section with two adaptive walls, the influence of the shear force was strong, and therefore it was possible to control the vertical dis placement of this section via the adaptive material. It was also pos sible to control the bending twist coupling of a non symmetric section through the variation of the shear centre.

As is evident, an increase in thickness of the section causes an increment of the stiffnesses of the section.

However, the influence of thickness on the ability to control such stiffnesses is not great; a thicker section results in a slight decrease. Therefore, effective control works robustly with respect to thickness changes.

By studying the variation of the thickness of the adaptive wall, it was observed that this variable strongly influences the position of shear centre of the section. Thus, if the thickness of the adaptive wall is changed, the bending twist coupling of the thin walled composite box beam analysed can also be controlled. This is possi ble when the section is not mechanically symmetrical, since in such a case the shear centre would always be situated at the same point.

References

[1] Raither W, Bergamini A, Gandhi F, Ermanni P. Adaptive bending–twist coupling in laminated composite plates by controllable shear stress transfer. Compos A 2012;43(10):1709–16.

[2] Kuder IK, Arrieta AF, Raither WE, Ermanni P. Variable stiffness material and structural concepts for morphing applications. Prog Aerosp Sci 2013;63:33–55.

[3] Ozdemir O, Kaya MO. Energy derivation and extension–flapwise bending vibration analysis of a rotating piezolaminated composite Timoshenko beam. Mech Adv Mater Struct 2014;21(6):477–89.

[4] Jovanović MM, Simonović AM, Zorić NZ, Lukić NS, Stupar SN, Ilić SS. Experimental studies on active vibration control of a smart composite beam using a PID controller. Smart Mater Struct 2013;22(11):115038.

[5] Choi SC, Park JS, Kim JH. Vibration control of pretwisted rotating composite thin-walled beams with piezoelectric fiber composites. J Sound Vib 2007;300 (1):176–96.

[6] Tawfik SA, Stefan Dancila D, Armanios E. Unsymmetric composite laminates morphing via piezoelectric actuators. Compos A 2011;42(7):748–56.

[7] Barbarino S, Bilgen O, Ajaj RM, Friswell MI, Inman DJ. A review of morphing aircraft. J Intell Mater Syst Struct 2011;22(9):823–77.

[8] Raither W, De Simoni L, Di Lillo L, Bergamini A, Ermanni P. Adaptive-twist airfoil based on electrostatic stiffness variation. SCITECH 2014, National Harbor; 2014.

[9] Gandhi F, Kang SG. Beams with controllable flexural stiffness. Smart Mater Struct 2007;16:1179–84.

[10] Raither W, Bergamini A, Ermanni P. Profile beams with adaptive bending–twist coupling by adjustable shear centre location. J Intell Mater Syst Struct 2013;24(3):334–46.

[11] Raither W, Heymanns M, Bergamini A, Ermanni P. Morphing wing structure with controllable twist based on adaptive bending–twist coupling. Smart Mater Struct 2013;22/6.

[12] Raither W. Adaptive-twist airfoils based on variable stiffness. PhD thesis. Swiss Federal Institute of Technology Zurich; 2014.

[13] Smith EC, Chopra I. Formulation and evaluation of an analytical model for composite box beams. J Am Helicopter Soc 1991;36(3):23–35.

[14] Kim NI, Shin DK. Coupled deflection analysis of thin-walled Timoshenko laminated composite beams. Comput Mech 2009;43(4):493–514.

[15] Volovoi VV, Hodges DH. Single-and multi-celled composite thin-walled beams. AIAA J 2002;40(5):960–5.

[16] Plusik A, Kollár LP. Torsion of closed section, orthotropic, thin-walled beams. Int J Solids Struct 2006;43(17):5307–36.

[17] Massa JC, Barbero E. Strength of materials formulation for thin walled composite beams with torsion. J Compos Mater 1997;32(17):1560–694.

[18] Rand O. Bending and extension of thin-walled composite beams of open cross-sectional geometry. J Appl Mech 2000;67(4):813–8.

[19] Barbero EJ. Introduction to composite materials design. 2nd ed. CRC Press; 2011.

[20] Kaddour AS, Hinton MJ, Smith PA, Li S. Mechanical properties and details of composite laminates for the test cases used in the third world wide failure exercise. J Compos Mater 2013;47(20–21):2427–42.